e-ISSN: 2667-4165 • CİLT / VOLUME: V • SAYI / ISSUE: I • HAZİRAN / JUNE 2022

AFYON KOCATEPE ÜNİVERSİTESİ ULUSLARARASI MÜHENDİSLİK TEKNOLOJİLERİ VE UYGULAMALI BİLİMLER DERGİSİ

Afyon Kocatepe University International Journal of Engineering Technology and Applied Sciences

www.dergipark.org.tr/tr/pub/akuumubd

AFYON KOCATEPE ÜNİVERSİTESİ
ULUSLARARASI MÜHENDİSLİK TEKNOLOJİLERİ ve UYGULAMALI BİLİMLER DERGİSİ
Afyon Kocatepe University
International Journal of Engineering Technology and Applied Sciences

Afyon Kocatepe University International Journal of Engineering Technology and Applied Sciences

http://dergipark.org.tr/akuumubd

e-ISSN:2667-4165

Afyon Kocatepe University
International Journal of Engineering Technology and Applied Sciences (AKU-IJETAS)

Volume: V / Number: 1 / December - 2022

Owner / Publisher: Prof. Dr. Ayhan EROL for Afyon Kocatepe University

Editor in Chief Prof. Dr. Ayhan EROL

Co- Editor in Chief Prof. Dr. Rıdvan ÜNAL

Published Afyon Kocatepe University, June 2022,

ijetas@aku.edu.tr

CONTACT INFORMATION

Afyon Kocatepe University International Journal of Engineering Technology and Applied Science Afyon Kocatepe University, Technology Faculty, 03200 Afyonkarahisar, TURKEY

Phone: +90-272-2281446 /ext.

Fax: +90-272 228 1449

e-mail : ijetas@aku.edu.tr, aerol@aku.edu.tr

Welcome to AKU-IJETAS

Dear Researchers;

Afyon Kocatepe University International Journal of Engineering and Applied Sciences ler has been published in Turkish and English since 2018 with 2 issues. Our journal will accept Turkish and English articles as 2 issues a year and the articles will be evaluated by at least two referees with the same system. Our magazine from December 2018; it offers many advantages to readers due to the practical and practical access to the authors as well as the process of publishing and publishing quickly and easily; The electronic journal (e-ISSN:2667-4165) accepts 2 numbers per year (June and December) in Turkish and English. The names of the judges evaluating the articles are not notified to the authors. The referees cannot see the names of the authors. The studies are evaluated as at least two referees. Our authors, who want to send articles, can register their original scientific articles online and follow the process by registering on our magazine page. Our journal is accepted as original and previously published research articles.

We are waiting for your contributions as both referee and writer. I thank you in advance for your support and I wish you success in your work.

Prof. Dr Ayhan EROL

Chief Editor

Danışma Kurulu / Editörler/ Editorial Board

Olga OROSOVA	Pavol Jozef Safarik University	SLOVAKIA
Otar ZUMBURIDZE	GeorgiaTechnical University	GEORGIA
P. Trinatha RAO	Gitam University	INDIA
Peter MONKA	Technical University Kosice	SLOVAKIA
Prasanna RAMAKRISNAN	Neo Education Institu	MALAYSIA
Ramazan KAÇAR	Karabük University	TURKEY
Radu COTETIU	Technical University Cluj Napoca	ROMANIA
Regita BENDIKIENĖ	Kaunas Technology University	LİTVANIA
Renata PANOCOVA	Pavol Jozef Safarik Üniversity	SLOVAKIA
Rıdvan UNAL	Afyon Kocatepe University	TURKEY
Robert CEP	Technical University Ostrava	CZECH
Serdar SALMAN	Marmara University	TURKEY
Serhat BASPINAR	Afyon Kocatepe University	TURKEY
Sermin OZAN	Fırat University	TURKEY
Sezai TAŞKIN	Celal Bayar University	TURKEY
Snezhina ANDONOVA	Sauth-West University	BULGARIA
Suleyman GUNDUZ	Karabük University	TURKEY
Stanislaw LEGUTKO	Poznan University of Technology	POLAND
Tomasz NIZNIKOWSKI	Lomza State University Applied Science	POLAND
Tomaz TOLLAZZI	Maribor University	SLOVENIA
Ugur CALIGULU	Firat University	TURKEY
Yılmaz YALCIN	Afyon Kocatepe University	TURKEY
Yuksel OĞUZ	Afyon Kocatepe University	TURKEY
Zoran TRIFUNOV	Mother Teresa University	MACEDONIA

CONTENTS

Page

Afyon Kocatepe Üniversitesi Uluslararası Mühendislik Teknolojileri ve Uygulamalı Bilimler Dergisi

Afyon Kocatepe University International Journal of Engineering Technology and Applied Sciences

AKÜ IJETAS Cilt **5(1)** (2022) Haziran (1-4 s) AKU J.Eng.App.Sci. **Vol 5(1)** (2022) June (1-4 pp)
DOI:10.53448/akuumubd.985577

Araştırma Makalesi / Research Article
e-ISSN 2667-4165 (https://dergipark.org.tr/akuumubd

CT Taramalarında Absorbe Edilen Dozun Hastanın Boyuna Göre Değişimi

İsmail Hakkı Sarpün[1,2,3], Timur Koca[3], Yasemin Şengün[3], Rahmi Atıl Aksoy[3], Ece Atak[3], Mehmet Kızılkaya[3], Aylin Fidan Korcum[3]

[1]*Akdeniz University, Physics Department, Antalya, Turkey*
[2]*Akdeniz University, Nuclear Sciences Application and Research Center, Antalya, Turkey*
[3]*Akdeniz University, Medicine Faculty, Radiation Oncology Department, Antalya, Turkey*

e-mail: sarpun@akdeniz.edu.tr. ORCID ID:http://orcid.org/0000-0002-9788-699X

The arrival date:21.08.2021 ; Date of Acceptance:08.02.2022

Anahtar Kelimeler
Keywords
CT;
Phantom;
NCICT;
Monte Carlo

Öz

Kanser tedavilerinde çekilen Bilgisayarlı Tomografi (CT) görüntüleri, tedavi portalı tasarımı ve planlamasında önemlidir. Hastanın CT taramalarında aldığı doz, tedavi planlaması doz hesaplamasında dikkate alınmaz ve kritik doz eşiğine sahip kritik organların sınır dozlarının hesaplanmasında önem kazanır. Bu çalışmada bazı kritik organlar olan kalp, karaciğer ve böbreklerin hastanın boyuna göre aldığı dozun değişimi Monte Carlo tekniği kullanılarak NCICT kodu ile araştırıldı. Sonuç olarak, dozlar hastaların boyuna göre değiştirildi.

Variation of the Dose Taken in CT Scanning According to the Height of the Patient

Keywords
Keywords
CT;
Phantom;
NCICT;
Monte Carlo

Abstract

Computed Tomography (CT) images taken in cancer treatments are important in treatment portal design and planning. The dose received by the patient in CT scans are not considered in the treatment planning dose calculation and becomes important in calculating the limit doses of the critical organs with critical dose threshold. In this study, the change of the dose received by some of the critical organs, namely the heart, liver, and kidneys, according to the height of the patient was investigated with the NCICT code using the Monte Carlo technique. As a result, doses were changed by the height of the patients.

1. Introduction

Despite providing major benefits for patients, CT is source of concern due to its potential radiation dose associated risks, especially for quite susceptible pediatric patients (National Research Council 2006). Epidemiological studies of cancer risk in CT patients require an estimate of the radiation dose absorbed by tissues within the x-ray exposed area (Sechopoulos *et al*. 2015).

Newer CT dosimetry codes have begun to include voxel phantoms (Zaidi and Xu 2007, Xu 2014, Caon 2004). If one compares with previous geometric phantoms, the voxel phantoms are represented more realistic anatomy, which is based on medical tomography images. While, WAZA-ARI, a web-based CT dose calculation system based on an adult male voxel phantom and PHITS code introduced by Ban *et al*. (2011), ImpactDose7, introduced by Kalender *et al*. (1999), is an

enhanced version of WinDose, and includes a set of both pediatric and adult voxel phantoms of ICRP (2009). VirtualDoseTMCT is a set of pediatric and adult configurable phantom-based software packages combined with GPU-based Monte Carlo simulation. Sahbaee *et al.* (2014) described a code based on a mathematical model derived from the correlation between coefficients of organ dose and patient body sizes.

Some of the mentioned codes are designed for the calculation of absorbed patient dose in large-scale clinical centers and are available as commercial. Calculation methods, which used in this study, were developed by Lee *et al*. (2015) to evaluate absorbed organ doses for CT patients, by using pediatric and adult reference voxel phantoms adopted by the ICRP and Monte Carlo simulation obtained from x-rays from CT examination.

2. Material and Method

The dose evaluation algorithm used by NCICT is based on the finding reported by Turner *et al*. (2010) that $CTDI_{vol}$ can be used as

$$D(\text{organ, age, gender,spectrum}) = \sum_{z=SS}^{z=SE} DC(\text{organ, age, gender, spectrum, } z) \times \text{CTDI}_{\text{vol}} \quad (1)$$

DC and $CTDI_{vol}$ parameters were expressed in Zaidi and Xu (2007), Sahbaee *et al.* (2014), Lee *et al*. (2015), Reiser *et al.* (2004), AAPM (2011) and if the $CTDI_{vol}$ is unknown, it could be evaluated via Eq. (2).

$$\text{CTDI}_{\text{vol}}(\text{make, model, spectrum}) = \frac{n\text{CTDI}_{\text{w}}(\text{make, model, spectrum})}{\text{Pitch}} \times \left(\frac{I \times t}{100}\right) \times k_{\text{OB}} \quad (2)$$

Organ absorbed dose per unit air kerma were calculated for Heart Wall, Liver and Kidney for adult female and male phantom (weight constant (80 kg), height variable) (Lee *et al.* 2012, Lee *et al.* 2011, Lee *et al.* 2014). Radiation exposure was simulated by selecting the predefined abdomen as the area for the 200 kV voltage of the irradiation geometry and the current-time value of 100 mAs. Fig. 1 shows the input screen used in the calculation and a female phantom weighing 80 kg with different heights.

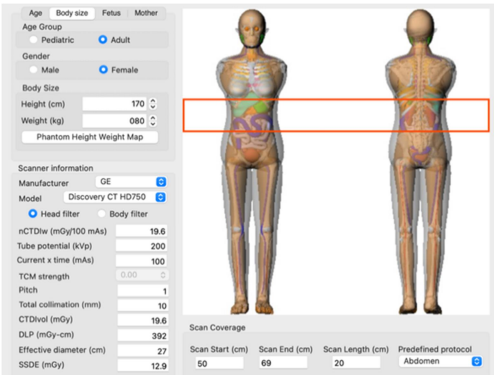

Figure 1. Female phantom weighing 80 kg with different heights

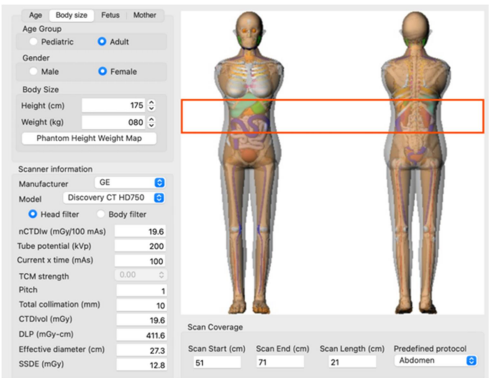

3. Calculations

By using phantoms (both male and female) weighing 80kg and different heights, the predefined abdominal region CT shots were simulated by selecting 200 kV tube voltage and 100 mAs current-time constant for a scanner most similar to the CT scanner in our clinic. Organ doses were calculated for Heart Wall, Liver and Kidney, which were determined as critical organs in the region. The variation of organ doses according to the phantom size is shown in Figs. 2 and 3.

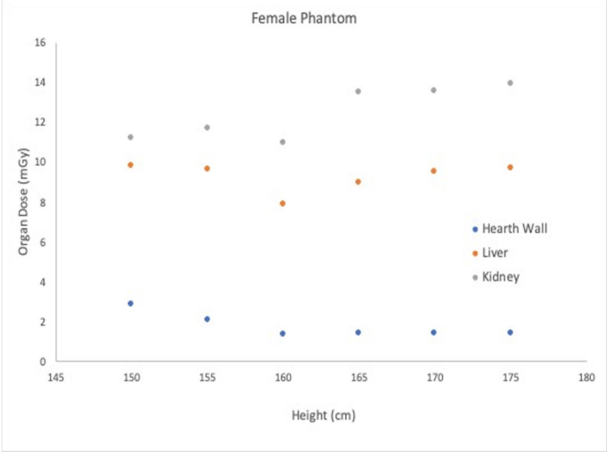

Figure 2. Variation of organ doses by height for 80 kg female phantom.

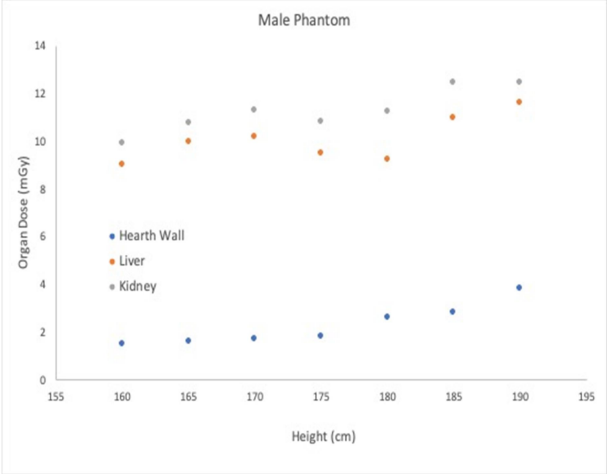

Figure 3. Variation of organ doses by height for 80 kg Male phantom.

The effective doses obtained by the same calculation are shown in Fig. 4.

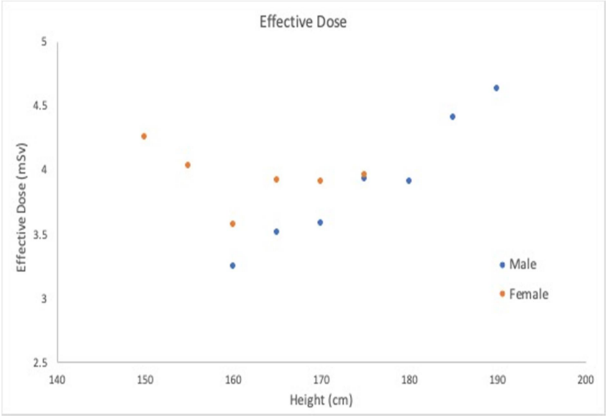

Figure 4. Variation of effective dose by height for both female and male phantoms.

4. Conclusion

The effective dose of the shot was calculated with Heart Wall, Liver and Kidney organ doses for both male and female phantoms with a mass of 80 kg and of different heights by using Monte Carlo-based NCICT code, with a tube voltage of 200 kV and a current-time value of 100 mAs in the pre-defined abdomen region irradiation in CT. Although organ doses for both phantoms increase with increasing height, when the effective doses are examined, despite the same relation being observed for the male phantom, there are irregularities in the values of the female phantom. Upon examination of organ doses and effective doses, irregular results are obtained with a length of 160 cm for the female phantom and a length of 175 cm for the male phantom. The obtained data will be beneficial for users employing ICRP phantoms for Monte Carlo dose calculation to compare the calculation process.

Acknowledgement

This study was partly presented at the ICETAS 2020 Conference.

References

AAPM, 2011. Size-specific dose estimates (ssde) in pediatric and adult body CT examinations. *AAPM Report* **204**, 1-30.

Ban, N., Takahashi, F., Sato, K., Endo, A., Ono, K., Hasegawa, T., Yoshitake, T., Katsunuma, Y. and Kai, M., 2011. Development of a web-based CT dose calculator: WAZA-ARI. *Radiation Protection Dosimetry*, **147**, 333–337.

Caon, M., 2004. Voxel-based computational models of real human anatomy: a review. *Radiation and Environmental Biophysics,* **42**, 229–35.

ICRP, 2009. Adult Reference Computational Phantoms ICRP Publication 110, *Annual ICRP,* **39,** 1–166.

Kalender, W.A., Schmidt, B. and Zankl, M., 1999. A PC program for estimating organ dose and effective dose values in computed tomography. *European Radiology,* **9**, 555–562.

Lee, E., Lamart, S., Little, M.P. and Lee, C., 2014. Database of normalised computed tomography dose index for retrospective CT dosimetry. *Journal of Radiological Protection*, **34,** 363–88.

Lee, C., Kim, K.P., Bolch, W.E., Moroz, B.E. and Folio, L., 2015. NCICT: a computational solution to estimate organ doses for pediatric and adult patients undergoing CT scans. *Journal of Radiological Protection*, **35,** 4, 891-909.

Lee, C., Kim, K.P., Long, D., Fisher, R., Tien, C., Simon, S.L., Bouville, A. and Bolch, W.E., 2011. Organ doses for reference adult male and female undergoing computed tomography estimated by Monte Carlo simulations. *Medical Physics*, **38,** 1196–206.

Lee, C., Kim, K.P., Long, D. and Bolch, W.E., 2012. Organ doses for reference pediatric and adolescent patients undergoing computed tomography estimated by Monte Carlo simulation. *Medical Physics*, **39,** 2129–46.

National Research Council, 2006. *Health Risks from Exposure to Low Levels of Ionizing Radiation: BEIR VII Phase 2*, Washington DC, National Academies Press.

Reiser, M.F., Takahashi, M., Modic, M. and Becker, C.R., 2004. *Multislice CT*, ed. Reiser, M.F., *et al*., Berlin, Springer.

Sahbaee, P., Segar, W.P. and Samei, E., 2014. Patient-based estimation of organ dose for a population of 58 adult patients across 13 protocol categories. *Medical Physics,* **41,** 072104.

missionZhang, D., Angel, E., Cody, D.D., Stevens, D.M., McCollough, C.H. and McNitt-Gray, M.F., 2010. The feasibility of a scanner-independent technique to estimate organ dose from MDCT scans: using $CTDI_{vol}$ to account for differences between scanners. *Medical Physics*, **37,** 1816.

Xu, X.G., 2014. An exponential growth of computational phantom research in radiation protection, imaging, and radiotherapy: a review of the fifty-year history. *Physics in Medicine and Biology,* **59**, R233–302.

Zaidi, H. and Xu, X.G., 2007. Computational anthropomorphic models of the human anatomy: the path to realistic Monte Carlo modeling in radiological sciences. *Annual Review of Biomedical Engineering*, **9**, 471–500

Afyon Kocatepe Üniversitesi Uluslararası Mühendislik Teknolojileri ve Uygulamalı Bilimler Dergisi

Afyon Kocatepe University International Journal of Engineering Technology and Applied Sciences

AKÜ IJETAS Cilt **5(1)** (2022) Haziran (5-12 s) AKU J.Eng.App.Sci. **Vol 5(1)** (2022) June (5-12 pp)
DOI:10.53448/akuumubd. 1116288

Araştırma Makalesi / Research Article
e-ISSN 2667-4165 (https://dergipark.org.tr/akuumubd

Karbon Nanotüp (KNT) İlave Edilmiş Poliakrilonitril (PAN) Nanoliflerin Elektroeğirme Yöntemi ile Üretilmesi ve Karakterizasyonu

Atike İnce Yardımcı[1], Yaser Açıkbaş[2,*]

[1]*Usak University, Technology Transfer Office, Usak, 64200, Turkey*
[2]*Usak University, Department of Materials Science and Nanotechnology Engineering, Usak, 64200, Turkey*

e-mail: atike.yardimci@usak.edu.tr, ORCID: 0000-0001-5482-4230
**e-mail: yaser.acikbas@usak.edu.tr, ORCID: 0000-0003-3416-1083*

The arrival date:13.05.2022 ; Date of Acceptance: 24.05.2022

Anahtar Kelimeler
Karbon Nanotüp (KNT);
Poliakrilonitril (PAN);
Elektroeğirme;
Nanolif;
Polimer Kompozit.

Öz

Bu çalışmada elektroeğirme yöntemi ile karbon nanotüp (KNT) ilave edilmiş poliakrilonitril (PAN) nanolif üretimi rapor edilmiştir. Boncuksuz ve düzenli PAN/KNT elektroeğirme yöntemi ile elde edilmiş nanofiberler elde etmek için beş farklı KNT konsantrasyonu (0.05, 0.1, 0.2, 0.5 ve %1 ağırlık) denenmiş ve nanolifleri karakterize etmek için Taramalı Elektron Mikroskobu (SEM), Raman ve X-Işını Difraksiyonu (XRD) analizleri kullanılmıştır. Sonuçlar, artan KNT konsantrasyonu ile PAN/KNT nanoliflerinin çapının arttığını ve optimum bir konsantrasyondan sonra nanolifler üzerinde bazı düzensiz bölgeler ve boncuklanmaların oluştuğunu göstermiştir. Bununla birlikte, KNT'lerin eklenmesi, PAN nanoliflerinin grafitizasyonunu ve kristalliğini arttırmıştır. Boncuksuz ve kristalizasyon seviyesi yüksek PAN/KNT nanolifler için optimum KNT konsantrasyonu ağırlıkça %0.1 olarak bulunmuştur.

Carbon Nanotube (CNT) Embedded Polyacrylonitrile (PAN) Electrospun Nanofibers Production and Characterizations

Keywords
Carbon Nanotube (CNT);
Polyacrilonitrile (PAN);
Electrospinning;
Nanofiber;
Polymer composite.

Abstract

Carbon nanotube (CNT) embedded polyacrylonitrile (PAN) nanofibers production by electrospinning method was reported in this study. Five different CNT concentrations (0.05, 0.1, 0.2, 0.5, and 1wt%) were tried to obtain beadless and regular PAN/CNT electrospun nanofibers. Scanning Electron Microscopy (SEM), Raman and X-Ray Diffaraction (XRD) analyses were utilized to characterize nanofibers. The results indicated that with increasing CNT concentration, the diameter of PAN/CNT nanofibers increased, and after an optimum concentration some disordered sites and beads were observed on the nanofibers. However, the addition of CNTs enhanced the graphitization and crystallinity of PAN nanofibers. The optimum CNT concentration for beadless and high crystalline PAN/CNT nanofibers was found as 0.1 wt%.

1. Introduction

For the fabrication of long organic fibers, electrospinning is a suitable electrostatic technique (Bhardwaj and Kundu 2010). In the electrospinning process, a sufficiently high voltage is needed to be applied to a liquid droplet in order to charge the body of the liquid (Li, Laurencin et al. 2002). This method could be utilized for the generation of porous, hollow and core-shell structures and allows for functionalization of the surface of nanofibers with various molecules and nanoparticles during or after the electrospinning process, as well. Nanofibers obtained with the electrospinning method with their excellent properties such as large surface area, small pore size, elasticity, high mechanical strength and biocompatibility are well-suited for many applications including actuators (Park, Gu et al. 2016), catalysts (Guerrero-Pérez 2021), air filtration (Yardimci, Kayhan et al. 2022), water purification (Ramakrishna, Jose et al. 2010, Chinnappan, Baskar et al. 2017), energy storage (Zhang, Kang et al. 2016), food applications (YARDIMCI and TARHAN , Kumar, Kumar et al. 2019), protective clothing (Gorji, Bagherzadeh et al. 2017), drug delivery (Son, Kim et al. 2014), tissue engineering (Ince Yardimci, Aypek et al. 2019, Ince Yardimci, Baskan et al. 2019), biosensors (Kivrak, Ince-Yardimci et al. 2020), and chemical sensors (Ince Yardimci, Yagmurcukardes et al. 2022).

Carbon nanotubes (CNTs) with the carbon-carbon sp^2 bonds they have display high stiffness and axial strength, and large Young modulus in their axial direction (Popov 2004). At the same time, they show extraordinary electrical conductivity and heat conductivity (Spitalsky, Tasis et al. 2010). They are appropriate nanomaterials to utilize for polymer composites. By adding CNTs to the polymer, their electrical and mechanical properties could be enhanced, the strength of the material could be increased and problematic creep could be decreased (Spinks, Mottaghitalab et al. 2006). By aligning CNTs to one direction, anisotropic mechanical and electrical properties could be obtained and especially along the alignment direction these properties improve dramatically (Zheng, Razal et al. 2011). In literature, CNTs were used with different polymers some of these polymers are epoxy (Kim, Seong et al. 2006), gel-coat (Yardimci, Tanoglu et al. 2013), polydimethylsiloxane (PDMS) (Jang, Yoon et al. 2021), polyvinylidene difluoride (PVDF) (Zhang and Vecitis 2014), poly(methyl methacrylate) (PMMA) (Yao, Wu et al. 2007), poly(vinyl alcohol) PVA (Jung, Cha et al. 2011) are some polymers utilized with CNTs.

In this study, we report the preparation of CNT embedded PAN nanofibers. Different CNT concentrations were investigated to obtain regular and beadless nanofibers and the results indicated that the generation of beadless PAN/CNT electrospun nanofibers with high crystallinity was achieved with the CNT concentration of 0.1 wt%.

2. Materials and Method

2.1. Materials

To produce PAN/CNT nanofibers PAN (MW=150000) was utilized as a polymer and N,N-dimethylformamide (DMF) was utilized as a solvent and they were purchased from Aldrich and used without further purification.

2.2 Preparation of PAN/CNT Solutions and Electrospinning Process

The process of CNT growth was presented in our previous work (Yardimci, Yılmaz et al. 2015). For PAN/CNT nanofibers production, the electrospinning method was used. To enhance the crystallinity of PAN, CNTs were inserted into the electrospinning solution in different amounts.

The applied voltage was changed between 15-25 kV and the flow rate of the solution was changed between 1.5 and 2.5 ml/h depending on solution viscosity and conductivity. The schematic of the electrospinning process is given in Fig. 1.

2.3 Characterization of PAN/CNT Electrospun Nanofibers

The morphology and diameter of PAN/CNT electrospun nanofibers were analysed by SEM. X-ray diffraction (XRD) studies using Cu Kα radiation source were utilized to understand the crystal phase of synthesized fibers and Raman spectroscopy was used with 514 nm Ar laser excitation to characterize the graphitic nature of pure PAN nanofibers and its CNT embedded forms.

3 Results and Discussions

SEM was utilized to characterize the surface morphology and diameter of pure PAN and PAN/CNT nanofibers. Fig. 2 displays the SEM micrographs of PAN nanofibers including the different amounts of CNT.

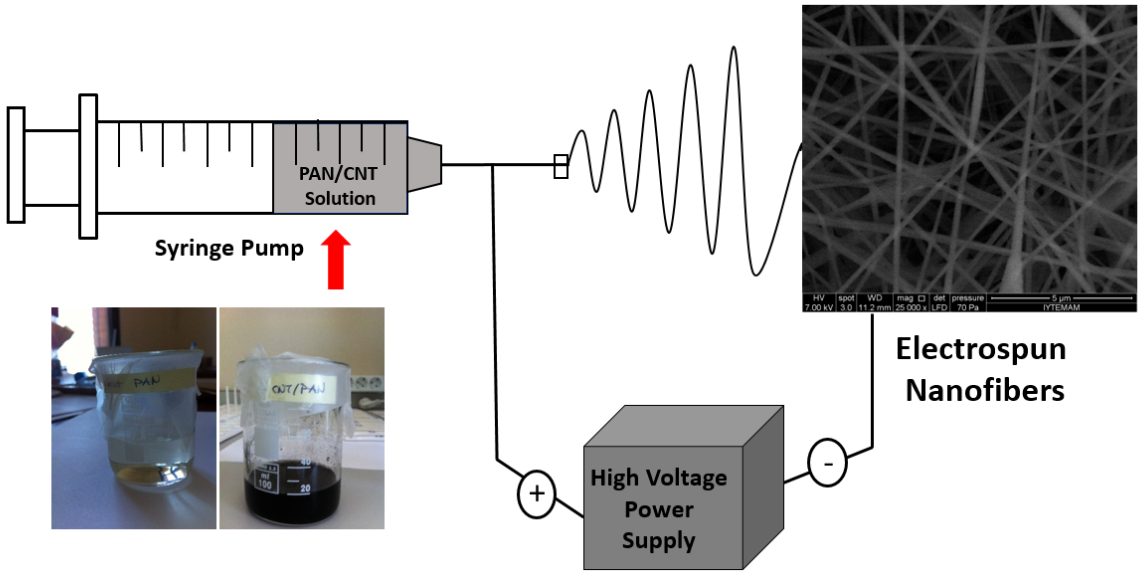

Figure 1 Schematic representation of electrospinning process.

It was observed that the fibers showed a smooth surface at low concentrations of CNTs, however with the increasing amount of CNT, especially at concentrations higher than 0.2 wt%, roughness increased dramatically. The reason for this roughness is CNT agglomeration and not embedded CNTs into the PAN nanofibers. Another effect of the increase in CNT concentration was observed on the diameter of nanofibers. The diameter of PAN nanofibers increased with increasing CNT concentration.

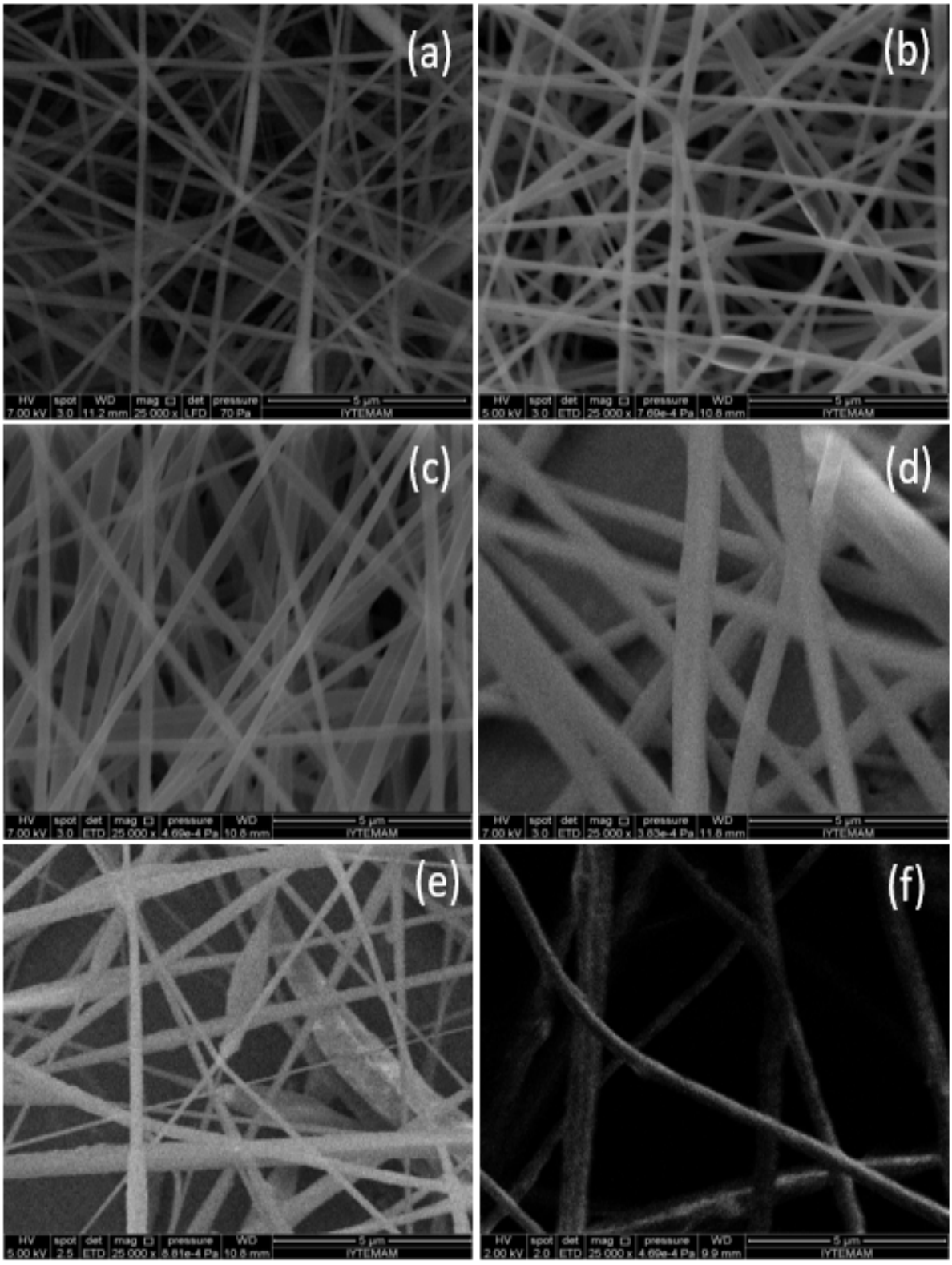

Figure 2 PAN/CNT nanofibers SEM images

While the average CNT diameter was about 83 nm for pure PAN nanofibers, this value increased to 405 nm for the sample including 1wt.% CNT as seen in Fig. 3. Diameters increased up to 0.5 wt% CNT loading, however at 0.5 wt% CNT amount, the average diameter decreased significantly. The reason for this change was probably because of the existence of beads on nanofibers. As expected, at 1 wt% CNT concentration the average diameter increased again.

XRD analysis was carried out in order to determine the improvement in graphitization in electrospun PAN nanofibers by adding CNT. XRD spectra obtained from PAN/CNT nanofiber are presented in Fig. 4. For the neat PAN nanofiber sheet, there was a strong peak at 29.95° which is relating to (020) crystal plane of PAN and a weak peak at 17.19° assigned to (200) crystal plane of PAN. The intensity of the peak of (200) crystal plane increased with increasing CNT concentration. CNT (002) at 27.2° and (004) at 54.4 ° crystal plane peaks (Kaur, Kumar et al. 2016) began to appear at 0.1 wt% CNT concentration and 0.5 wt% CNT concentrations, respectively. These CNT peaks appearance indicates better crystallinity than neat PAN nanofibers.

Fig. 5 displays Raman spectra of the electrospun PAN nanofibers. For neat PAN nanofibers, it was observed only the Raman scattering peak of the nitrile group (-CN) at 2240 cm^{-1} (Matsuno, Takagaki et al. 2020). With CNT addition, this peak intensity began to decrease and at high CNT concentrations, this peak disappeared. D-band at ~1370 cm^{-1} and G-band at ~1590 cm^{-1} of CNTs were observed at 0.2 and 0.5 wt% of CNT concentrations (Dresselhaus, Dresselhaus et al. 2005). With increasing CNT concentrations I_G/I_D value of electrospun nanofibers also increased. This Raman data support XRD results; graphitization increased with increasing CNT concentration.

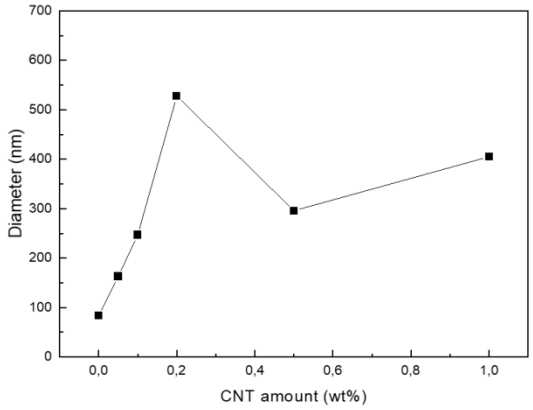

Figure 3 Average diameter distribution of PAN/CNT electrospun nanofibers.

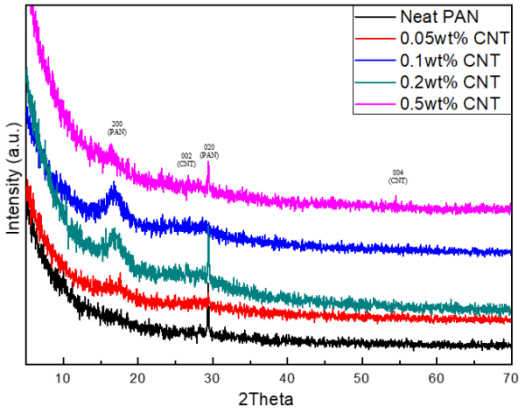

Figure 4 XRD scans of CNT embedded PAN electrospun nanofibers.

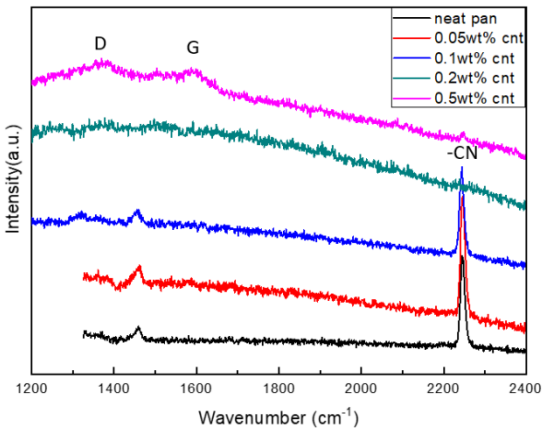

Figure 5 Raman spectra of CNT embedded PAN electrospun nanofibers.

4. Conclusions

In conclusion, PAN/CNT nanofibers containing different amounts of CNT were prepared through the electrospinning method. The results indicated that CNT addition enhanced the crystallinity and graphitization of PAN nanofibers. However, SEM pictures showed that the size of electrospun nanofibers was firstly became thicker and then their morphology and shape began to deteriorate with increasing CNT concentration. Bead formation on nanofibers and some irregulars in the nanofiber morphology were observed at high CNT concentrations. Overall, the optimum CNT concentration was found as 1 wt% and the average diameter of nanofibers obtained by using this concentration of CNT was measured as 248 nm.

5. References

Bhardwaj, N. and S. C. Kundu, (2010). Electrospinning: a fascinating fiber fabrication technique. *Biotechnology advances* **28**(3): 325-347.

Chinnappan, A., et al. (2017). An overview of electrospun nanofibers and their application in energy storage, sensors and wearable/flexible electronics. *Journal of Materials Chemistry C* **5**(48): 12657-12673.

Dresselhaus, M. S., et al. (2005). Raman spectroscopy of carbon nanotubes. *Physics reports* **409**(2): 47-99.

Gorji, M., et al. (2017). Electrospun nanofibers in protective clothing. *Electrospun nanofibers*, *Elsevier***:** 571-598.

Guerrero-Pérez, M. O. (2021). "Research progress on the applications of electrospun nanofibers in catalysis." Catalysts **12**(1): 9.

Ince Yardimci, A., et al. (2019). CNT incorporated polyacrilonitrile/polypyrrole nanofibers as keratinocytes scaffold. *Journal of Biomimetics, Biomaterials and Biomedical Engineering*, Trans Tech Publ.

Ince Yardimci, A., et al. (2019). Osteogenic differentiation of mesenchymal stem cells on random and aligned PAN/PPy nanofibrous scaffolds. *Journal of biomaterials applications* **34**(5): 640-650.

Ince Yardimci, A., et al. (2022). Electrospun polyacrylonitrile (PAN) nanofiber: preparation, experimental characterization, organic vapor sensing ability and theoretical simulations of binding energies. *Applied Physics A* **128**(3): 1-12.

Jang, D., et al. (2021). Improved electric heating characteristics of CNT-embedded polymeric composites with an addition of silica aerogel. *Composites science and technology* **212**: 108866.

Jung, E. H., et al. (2011). Electrical conductive CNT-PVA/PC nanocomposites with high tensile elongation. *Journal of nanoscience and nanotechnology* **11**(1): 597-601.

Kaur, N., et al. (2016). Synthesis and characterization of multiwalled CNT–PAN based composite carbon nanofibers via electrospinning. *SpringerPlus* **5**(1): 1-7.

Kim, J. A., et al. (2006). Effects of surface modification on rheological and mechanical properties of CNT/epoxy composites. *Carbon* **44**(10): 1898-1905.

Kivrak, E., et al. (2020). Aptamer-based electrochemical biosensing strategy toward human non-small cell lung cancer using polyacrylonitrile/polypyrrole nanofibers. *Analytical and Bioanalytical Chemistry* **412**(28): 7851-7860.

Kumar, T. S. M., et al. (2019). A comprehensive review of electrospun nanofibers: Food and packaging perspective. *Composites Part B: Engineering* **175**: 107074.

Li, W. J., et al., (2002). Electrospun nanofibrous structure: a novel scaffold for tissue engineering. *Journal of biomedical materials research* **60**(4): 613-621.

Matsuno, R., et al. (2020). Relationship between the Relative Dielectric Constant and the Monomer Sequence of Acrylonitrile in Rubber. *ACS omega* **5**(26): 16255-16262.

Park, J.-M., et al., (2016). Mechanical and electrical properties of electrospun CNT/PVDF nanofiber for micro-actuator applications. *Advanced Composite Materials* **25**(4): 305-316.

Popov, V. N. (2004). Carbon nanotubes: properties and application. *Materials Science and Engineering: R: Reports* **43**(3): 61-102.

Ramakrishna, S., et al. (2010). Science and engineering of electrospun nanofibers for advances in clean energy, water filtration, and regenerative medicine. *Journal of Materials Science* **45**(23): 6283-6312.

Son, Y. J., et al. (2014). Therapeutic applications of electrospun nanofibers for drug delivery systems. *Archives of pharmacal research* **37**(1): 69-78.

Spinks, G. M., et al. (2006). Carbon-Nanotube-Reinforced Polyaniline Fibers for High-Strength Artificial Muscles. *Advanced Materials* **18**(5): 637-640.

Spitalsky, Z., et al. (2010). Carbon nanotube–polymer composites: chemistry, processing, mechanical and electrical properties. *Progress in polymer science* **35**(3): 357-401.

Yao, X., et al., (2007). Carbon nanotube/poly (methyl methacrylate)(CNT/PMMA) composite electrode fabricated by in situ polymerization for microchip capillary electrophoresis. *Chemistry–A European Journal* **13**(3): 846-853.

Yardimci, A. I., et al., (2022). Synthesis and air permeability of electrospun PAN/PVDF nanofibrous membranes. *Research on Engineering Structures and Materials*.

Yardimci, A. I., et al., (2013). Development of electrically conductive and anisotropic gel-coat systems using CNTs. *Progress in Organic Coatings* **76**(6): 963-965.

Yardimci, A. İ. and Ö. TARHAN ELECTROSPUN PROTEIN NANOFIBERS AND THEIR FOOD APPLICATIONS. *Mugla Journal of Science and Technology* **6**(2): 52-62.

Yardimci, A. I., et al., (2015). The effects of catalyst pretreatment, growth atmosphere and temperature on carbon nanotube synthesis using Co–Mo/MgO catalyst. *Diamond and Related Materials* **60**: 81-86.

Zhang, B., et al., 2016. Recent advances in electrospun carbon nanofibers and their application in electrochemical energy storage. *Progress in Materials Science* **76**: 319-380.

Zhang, Q. and C. D. Vecitis, 2014. Conductive CNT-PVDF membrane for capacitive organic fouling reduction. *Journal of Membrane Science* **459**: 143-156.

Zheng, W., et al., 2011. Artificial muscles based on polypyrrole/carbon nanotube laminates. *Advanced materials* **23**(26): 2966-2970.

Afyon Kocatepe Üniversitesi Uluslararası Mühendislik Teknolojileri ve Uygulamalı Bilimler Dergisi

Afyon Kocatepe University International Journal of Engineering Technology and Applied Sciences

AKÜ IJETAS Cilt **5(1)** (2022) Haziran (13-17 s) AKU J.Eng.App.Sci. **Vol 5(1)** (2022) June (13-17 pp)
DOI:10.53448/akuumubd. 1111800

Araştırma Makalesi / Research Article
e-ISSN 2667-4165 (https://dergipark.org.tr/akuumubd

Asimetrik Michael Katılma Tepkimesi için Prolin bazlı β-Hidroksiamit Organokatalizörü

Selahattin Bozkurt[1,2]
[1] Scientific Analysis Technological Application and Research Center, Usak University, 64200 Usak, Turkey.
[2] *Vocational School of Health Services, Usak University, 64200 Usak, Turkey.*

e-posta: selahattin.bozkurt@usak.edu.tr. ORCID ID://orcid.org/0000-0002-9147-5938

Geliş Tarihi:30.04.2022 ; Kabul Tarihi:02.06.2022

Anahtar kelimeler
Michael katılması; Organokatalizör; Enantiyomerik aşırılık; *L*-Prolin.

Özet

Michael katılması gibi C-C bağı oluşturma yeteneğine sahip reaksiyon tiplerinde, kiral organokatalizör uygulamaları son yılların önemli araştırma alanlarındandır. Organik reaksiyon tiplerinden önemli çalışmalarından biri olan Michael katılmasına en iyi örneklerden biri de organokatalizörler varlığında nitroolefinlerin ketonlar ile reaksiyonudur. Bu çalışmada; *L*-prolin bazlı amit türevi, ılımlı bir verim ile sentezi gerçekleştirilmiş ve yapısı çeşitli teknikler ile aydınlatılmıştır. Sentezi gerçekleştirilen bu bileşiğin; organokatalizör olarak, Michael katılma çalışmalarında enantiyomerik aşırılık (e.e.) üzerine etkisi incelenmiş ve en iyi enantiyomerik aşırılık değerinin karbontetra klorür (CCl_4) içinde ve %65 olduğu tespit edilmiştir.

Prolines Based β-Hydroxyamide as Organocatalysts for Use in Asymmetric Michael Addition

Keywords
Michael addition; Organocatalyst; Enantiomeric excess; *L*-Proline.

Abstract

Applications of chiral organocatalysts in reaction types capable of forming C-C bonds, such as Michael addition, are one of the important research areas of recent years. One of the best examples of Michael addition, one of the important works of organic reaction types, is the reaction of nitroolefins with ketones in the presence of organocatalysts. In this study, *L*-proline-based amide derivative was synthesized with moderate yield and its structure was elucidated by various techniques. As an organocatalyst, its effect on enantiomeric excess (e.e.) was investigated in Michael addition studies and the best enantiomeric excess value was found to be 65% in carbontetra chloride (CCl_4).

1. Introduction

The use of stereoisomeric pure compounds in many industrial sectors such as pharmaceutical production is an issue that needs attention. (Bulger 2012) To obtain such compounds, scientists have studied many different methods. One of these studies is the use of organocatalysts in the production of pure stereoisomeric compounds. Organocatalysts, besides offering an effective and very useful way (Barrulas al 2014) both in industry and in research (Carlone al 2019), are among the most popular areas of recent interest with their low toxic effect (Susam al 2021). Organocatalysts are of interest because they are easy to obtain, inexpensive and environmentally friendly. (Dalko al. 2004, List 2006) As a matter of fact, the Nobel

Prize in chemistry in 2021 was given to two scientists who worked on asymmetric organocatalysts. Asymmetric organocatalysts have a valuable place in the synthesis of chiral organic molecules. (List 2004) The use of organocatalysts in reactions carried out to obtain chiral molecules with high enantiopurities makes the use of such catalysts important (Bozkurt 2008).

Organocatalysts consisting of enantiopure groups such as *L*-Proline are used in many reactions such as aldol condensation (Liu 2010), Michael addition (Jin 2016, Zhiwei 2022), Mannich reactions (Kumar 2019).

Michael addition, which is one of the useful reactions for the formation of C-C bonds, involves the addition of a nucleophile to the molecule with an electron withdrawing group (Castan 2018). In these reaction studies, obtaining an addition product with enantiopurity, thanks to the use of organocatalyst, is rather a young subject. An important example of these reactions is the addition of aldehyde (Durmaz 2013, Naziroglu 2012) or ketone (Vural 2016) to nitroolefins. The conversion of compounds containing nitro group to amine, nitrile oxide oxide, carbonyl with various synthetic steps increases the importance of these compounds even more (Shim 2020).

L-proline and its derivatives emerge as important chiral organocatalysts used in Michael addition reactions. In the literature, the use of different chiral organocatalysts has been encountered with the attachment of compounds such as diarylprolinol silylether (Zhu al 2010), proline lithium salt (Xu 2013), pyrrolidine-based triazole (Yan 2006) and pyrrolidine-based imidazole (Yumiko 2018) to the main skeleton of proline. As the formation of this reaction; It is predicted that first of all, an imine/enamine is formed between the ketone/aldehyde derivatives and the nitrogen atom of the prolidine, followed by the incorporation of nitroolefins into this imine (Michael 2015). The presence of various hydrogen donor and acceptor groups, as well as bulky groups with steric hindrance, in the structure of the enantiopure organocatalyst; causes nitroolefins to attack from a preferential direction (Hong 2021). In this case, the product to be formed allows the formation of an enantiomerically rich product. For the reasons mentioned above, we designed a new organocatalyst based on prolidine and containing bulky groups as well as hydrogen acceptor-donor groups in its structure.

2. Experimental

2.1 General

Melting points were determined on an Electrothermal 9100 apparatus in a sealed capillary. ^{1}H and ^{13}C NMR spectra were recorded at room temperature on a Varian 400 MHz spectrometer in $CDCl_3$. IR spectra were obtained on a Perkin Elmer FTIR spectrum-100 FTIR spectrometer using ATR. Optical rotations were measured on an Atago AP-100 digital polarimeter. The HPLC measurements were carried out on Agilent 1100 equipment connected with chiral column. Elemental analyses were performed using a Leco CHNS-932 analyzer.

Analytical TLC was performed using Merck prepared plates (silica gel 60 F_{254} on aluminum). Flash chromatography separations were performed on a Merck Silica Gel 60 (230-400 Mesh). All reactions, unless otherwise noted, were conducted under a nitrogen atmosphere. All starting materials and reagents used were of standard analytical grade from Fluka, Merck and Aldrich and used without further purification. Toluene was distilled from CaH_2 and stored over sodium wire. Other commercial grade solvents were distilled, and then stored over molecular sieves. The drying agent employed was anhydrous $MgSO_4$.

2.2 Syntheses

The synthesis of **Compound I** has been already described by us. (Bozkurt *al*. 2012)

2.2.1 Synthesis of benzyl (S)-2-(((S)-3-(dibenzylamino)-2-hydroxypropyl) carbamoyl) pyrrolidine-1-carboxylate (Compound II)

To a cooled solution of DCC (206 mg, 1 mmol) in CH_2Cl_2 (5 mL) was slowly added to a solution of N-Benzyloxycarbonyl-*L*-proline (260 mg, 1 mmol) in CH_2Cl_2 (5 mL) at 0 °C. Stirred the reaction for an hour. Then, optically pure Amine **I** (1.15) in CH_2Cl_2 (5 mL) was added dropwise and the resulting solution was stirred for 24 h. Then, CH_2Cl_2 (10 mL)

was added and filtrated, the solvent was removed under reduced pressure and the crude product was purified by flash chromatography on silica gel ($CHCl_3$/MeOH 20:1 as eluent) to afford **Compound II**. Viscous yellow oil, yield 79%; $\propto_D^{25}$= + 8.2 (c 0.74, $CHCl_3$); ^{1}H-NMR (400 MHz, *CDCl*$_3$): δ (ppm) 7.54–7.13 (m, 15H, Ar*H*), 6.59 (bs, 1H, N*H*), 5.26–4.97 (m, 2H, OCH_2Ar), 4.32–4.00 (m, 1H, NC*H*), 3.89–3.61 (m, 3H, C*H*OH and NCH_2), 3.57–3.32 (m, 5H, NCH_2, NCH_2, O*H*), 3.19–2.72 (m, 2H, NCH_2), 2.63–2.27 (m, 2H, NCH_2), 2.20–1.76 (m, 4H, C*H*CH_2, CH_2CH_2); 13C-NMR (100 MHz, *CDCl*$_3$) δ (ppm) 172.7, 154.3, 139.1, 136.1, 130.0, 128.4, 128.2, 127.9, 127.6, 127.3, 71.5, 67.2, 58.1, 56.8, 46.4, 41.2, 29.1, 20.5; Anal. Calcd for $C_{30}H_{35}N_3O_4$ (501.32): C, 71.83%; H, 7.03%; N, 8.38%; Found C, 71.79%; H, 7.04%; N, 8.39%.

Synthesis of (S)-N-((S)-3-(dibenzylamino)-2-hydroxypropyl)pyrrolidine-2-carboxamide (Compound III)

To a solution of **Compound II** (1.0 mmol) in ethanol (15 mL) was added Pd/C (156 g) and cyclohexene (0.5 mL). The mixture was refluxed for 3 h. After the completion of the reaction, the solution was cooled to rt, filtered on Celite to remove any solids, the solvent was removed under reduced pressure and the residue was chromatographed on a silica gel column to obtain pure **Compound III**. Viscous yellow oil, yield 43%; $\propto_D^{25}$= + 10.2 (c 1.11, $CHCl_3$); ^{1}H-NMR (400 MHz, C*D*Cl_3): δ (ppm) 7.60 (t, *J* = 5.04 Hz, 1H, N*H*), 7.40–7.04 (m, 10H, Ar*H*), 3.86–3.66 (m, 3H, C*H*OH and NCH_2Ar), 3.49 (dd, *J* = 9.14, 5.46 Hz, 1H, NHCH_2), 3.41–3.23 (m, 3H, NHCH_2 and NCH_2Ar), 3.08 (ddd, *J* = 13.84, 6.54, 5.46 Hz, 1H, NHCH_2), 2.89–2.74 (m, 2H, NHC$H_2CH_2CH_2$), 2.41–2.27 (m, 3H, NCH_2CH and O*H*), 2.00 (tdd, *J* = 12.72, 9.10, 7.38, 7.38 Hz, 2H, CHCH_2CH_2), 1.72 (td, *J* = 19.27, 6.21, 6.21 Hz, 1H, CHCH_2CH_2), 1.66–1.54 (m, 2H, $CHCH_2CH_2$). ^{13}C-NMR (100 MHz, C*D*Cl_3) δ (ppm) 171.3, 138.6, 128.8, 128.2, 127.2, 68.7, 63.1, 61.4, 58.7, 46.3, 45.9, 30.7, 25.5; Anal. Calcd for $C_{22}H_{29}N_3O_2$ (367.28): C, 71.90%; H, 7.95%; N, 11.43%; Found C, 71.88%; H, 7.94%; N, 11.44%.

General Experimental Procedure for the Michael Addition of Cyclohexanone to Nitroolefins

To a mixture of catalyst (0.0025 mmol), nitroolefin (0.25 mmol) in carbontetrachloride (0.250 mL) was added the carbonyl compound (1.5 mmol). The reaction mixture was stirred at room temperature until the nitroolefin was completely consumed (monitored by TLC). After evaporation of the solvent under vacuum, the residue was separated by flash chromatography over silica gel (hexane/ethyl acetate = 10:1) to give the Michael adduct. The enantiomeric excess was determined by chiral HPLC with OD-H columns.

3. Result and Discussion

The synthesis of organocatalysts containing hydrogen donor-acceptor groups and bulky groups capable of pi-pi interaction is extremely important in obtaining enantiomerically rich compounds. In our previous studies, we obtained an amino alcohol derivative with two separate phenyl groups in its structure to contain it in bulky groups. To obtain an important derivative of these compounds; In this study, we synthesized a new proline amide as a result of the reaction of amine group protected *L*-proline with an amino alcohol derivative.

Compound I, prepared according to the procedures previously described by us, was treated with the enantiopure *L*-(-)-Cbz-protected proline in the presence of DCC (Dicyclohexylcarbodiimide) in dry CH_2Cl_2. Later on; Compound III is obtained as the final product by boiling it in a solution in ethanol in the presence of Pd/C (10%) and cyclohexane to remove the CBZ protecting group in the structure of Compound II in moderate yield as shown in *Scheme 1*. All products structures were determined by appropriate spectroscopic techniques such as ^{1}H-NMR, ^{13}C NMR.

When the ^{1}H NMR spectrum of Compound III was examined, it was observed that the amide proton resonated as a triplet at 7.60 ppm, while the NHCH_2 protons resonated as a doublet of a doublet of a doublet at 3.49 ppm. On the other hand, it was determined that CHOH protons formed multiplet-shaped peaks between 3.49–3.59 ppm. Moreover; It was observed that aromatic protons had multiplet resonance between 7.40–7.04 ppm.

To investigate the efficiency of the obtained proline amide derivative as a chiral organocatalyst; As a model reaction, on different solvents, the

reaction between cyclohexanone and β-nitrostyrene was studied. As can be seen in *Table 1*, first of all, the addition study in water was carried out. However, both the yield of the product formed and the yield of enantiopurity were not at the desired level.

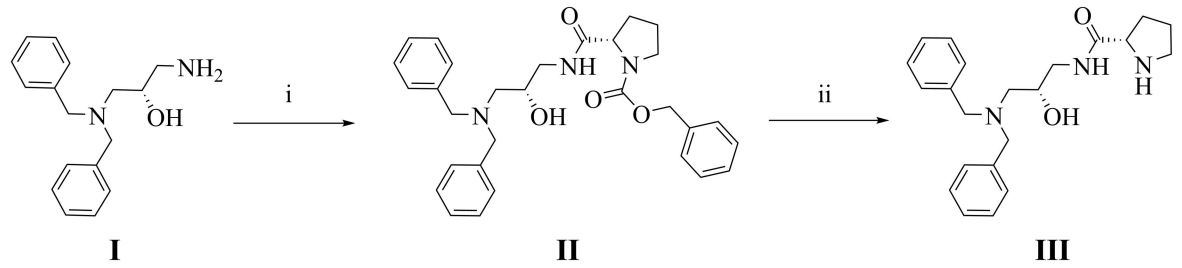

Scheme 1. (i) DCC, Cbz-*L*-Proline, CH_2Cl_2, rt; (ii)Pd/C, cyclohexene, ethanol, reflux.

Then the same reaction; When repeated in different solvent environments, the product is obtained in both THF and chloroform with a yield of 75%; It was observed that the ee value reached 56% and 63% in these solvents, respectively.

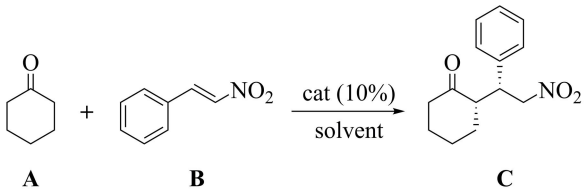

Table 1. Asymmetric Michael addition of cyclohexanone to trans-β-nitrostyrene

Entry	Solvent	Time (d)	Yield (%)[a]	d.r.[b]	e.e. (%)[c]
1	H_2O	3	38	99/1	13
2	H_2O+DMSO	3	40	99/1	18
3	THF	3	75	99/1	56
4	$CHCl_3$	3	75	99/1	63
5	CCl_4	3	80	99/1	64
6	Toluene	3	70	nd	nd

4. Conclusions

In conclusion, we synthesized a new chiral β-hydroxyamide-pyrrolidine-based catalysts for the Michael addition reaction of cyclohexanone with β-nitrostyrene. Moderate yields, high diastereoselectivities, and modarate enantioselectivities were achieved.

Acknowledgement

The author would like to thank Prof. Dr. Abdulkadir Sırıt for support during the preparation this study.

5. References

Bulger, P.G., 2012. Industrial Applications of Organocatalysis, Editor(s): Erick M. Carreira, Hisashi Yamamoto, Comprehensive Chirality, Elsevier, 228-252.

Barrulas, P.C., Genoni, A., Benaglia, M., Burke A.J., 2014. Cinchona-Derived Picolinamides: Effective Organocatalysts for Stereoselective Imine Hydrosilylation. *Eur. J. Org. Chem.* 7339–7342.

Carlone, A. and Bernardi, L. 2019. Enantioselective organocatalytic approaches to active pharmaceutical ingredients – selected industrial examples *Physical Sciences Reviews*, **4**, 20180097.

Susam, Z.D., Tanyeli, C., 2021, Recyclable Organocatalysts in Asymmetric Synthesis. *Asian Journal of Organic Chemistry*, **10**, 1251-1266.

Dalko, P.I., Moisan, L. 2004, In the golden age of organocatalysis. *Angewandte Chemie International Edition*., **43**, 5138–5175.

List, B., 2006. The ying and yang of asymmetric aminocatalysis. *Chemical Communications*. 819–824.

https://www.nobelprize.org/prizes/chemistry/2021/press-release/ (20.04.2022)

List, B., 2004. Organocatalysis: a complementary catalysis strategy advances organic synthesis. *Advanced Synthesis & Catalysis,* **346,** 1021.

Bozkurt, S., Durmaz, M., Yilmaz, M., Sirit, A., 2008. Calixarene-based chiral phase-transfer catalysts derived from cinchona alkaloids for enantioselective synthesis of α-amino acids. *Tetrahedron: Asymmetry* **19**, 618-623.

Liu, L., Liu, ZT., Liu, ZW. et al. 2010. *L*-Proline catalyzed aldol reactions between acetone and aldehydes in supercritical fluids: An environmentally friendly reaction procedure. *Sci. China Chem.* **53**, 1586–1591.

Jin, H., Kim, S.T., Hwang, G.S., Ryu, D.H., 2016. *L*-Proline Derived Bifunctional Organocatalysts:

Enantioselective Michael Addition of Dithiomalonates to trans-β-Nitroolefins. *The Journal of Organic Chemistry* **81**, 3263-3274.

Kumar, GR., Ramesh, B., Yarlagadda, S., Sridhar, B., Reddy, B.V.S, 2019. Organocatalytic Enantioselective Mannich Reaction: Direct Access to Chiral β-Amino Esters. *ACS Omega* **4**, 2168-2177.

Castan, A. Badorrey, R., Galvez J.A., Lopez-Ram-de-Viu, P., DiazVillegasde, M.D., 2018. Michael addition of carbonyl compounds to nitroolefins under the catalysis of new pyrrolidine-based bifunctional organocatalysts. *Organic & Biomolecular Chemistry* **16**, 924-935

Durmaz, M., Sirit, A. 2013. Application of L-prolinamides as highly efficient organocatalysts for the asymmetric Michael addition of unmodified aldehydes to nitroalkenes. *Supramol. Chem.* **25**, 292–301.

Naziroglu, H.N., Durmaz, M., Bozkurt, S., Demir, A.S., Sirit, A. 2012. Application of L-prolinamides as highly efficient organocatalysts for the asymmetric Michael addition of unmodified aldehydes to nitroalkenes. *Tetrahedron: Asymmetry* **23**, 164-169.

Vural, U., Durmaz, M., Sirit, A. 2016. A novel calix [4] arene-based bifunctional squaramide organocatalyst for enantioselective Michael addition of acetylacetone to nitroolefins. *Organic Chemistry Frontiers* **3**, 730-736.

Shim, J.H., Lee, M.J., Lee, M.H., Kim, B.,S., Ha, D.C., 2020. Enantioselective organocatalytic Michael reactions using chiral (R,R)-1,2-diphenylethylenediamine derived thioureas. *RSV Adv*. **10**, 31808.

Zhu, S., Yu, S., Wang, Y. and Ma, D. 2010. Organocatalytic Michael Addition of Aldehydes to Protected 2-Amino-1-Nitroethenes: The Practical Syntheses of Oseltamivir (Tamiflu) and Substituted 3-Aminopyrrolidines*. Angew. Chem. Int. Ed.,* **49,** 4656-4660.

Xu, K., Zhang, S., Hu, Y., Zha, Z. and Wang, Z. 2013. Asymmetric Michael Reaction Catalyzed by Proline Lithium Salt: Efficient Synthesis of L-Proline and Isoindoloisoquinolinone Derivatives. *Chem. Eur. J.,* **19**, 3573-3578.

Yan, Z.Y., Niu, Y.N., Wei, H.L., Wu, L.Y., Zhao, Y.B., Liang, M. 2006. Combining proline and 'click chemistry': a class of versatile organocatalysts for the highly diastereo- and enantioselective Michael addition in water. *Tetrahedron: Asymmetry* **17**, 3288-3293.

Yumiko, S., 2018. Asymmetric Michael Addition Mediated by Chiral Ionic Liquids. *Mini-Reviews in Organic Chemistry* **15**, 236-245.

Michael, H., Haindl, M.H., Hioe, J., Gschwind, R.M., 2015. The Proline Enamine Formation Pathway Revisited in Dimethyl Sulfoxide: Rate Constants Determined via NMR*. Journal of the American Chemical Society* **137**, 12835-12842.

Hong, H., Wang, H., Zheng, C., Zhao, G., Shang, Y., 2021. Organophosphine bearing multiple hydrogen-bond donors for asymmetric Michael addition reaction of 1-oxoindane-2-carboxylic acid ester via dual-reagent catalysis. *Chinese Chemical Letters*, **32**, 708-712.

Bozkurt, S., Yilmaz, M., Sirit, A., 2012. Chiral Calix[4]arenes Bearing Amino Alcohol Functionality as Membrane Carriers for Transport of Chiral Amino Acid Methylesters and Mandelic Acid. *Chirality*, **24**, 129-136

AFYON KOCATEPE ÜNİVERSİTESİ ULUSLARARASI MÜHENDİSLİK TEKNOLOJİLERİ ve UYGULAMALI BİLİMLER DERGİSİ

Afyon Kocatepe Üniversitesi
Ahmet Necdet Sezer Kampüsü
Teknoloji Fakültesi
AFYONKARAHİSAR
Tel: +90 272 228 14 46
Belgegeçer: +90 272 228 14 49
E-posta: ijetas@aku.edu.tr

www.ijetas.aku.edu.tr